EFFECT OF FLARE ANGLE AND NATURAL VENTILATION ON THE AERODYNAMIC CHARACTERISTICS OF A TYPICAL RE-ENTRY BODY AT SUBSONIC AND TRANSONIC MACH NUMBERS

G.K. Suryanarayana
Scientist
National Aerospace Laboratories (NAL)
Council of Scientific and Industrial Research (CSIR)
Kodihalli, Post Box No. 1779
Bangalore-560 017, India
Email : surya@nal.res.in

Abstract

Aerodynamic force and moment measurements were carried out on models of a typical re-entry body, featuring a blunt nose, conical body and flare, to assess the effect of flare angle on the overall aerodynamic characteristics. In one of the configurations, the junction between the cone and the flare was vented out to the base of the model to assess the effect of ventilation on the aerodynamic characteristics. It was expected that the stability characteristics would improve, by virtue of improved contribution from the flare to the normal force of the configuration. However, measurements did not show the expected trends. Instead, there was a remarkable reduction in the axial force with ventilation, by as much as 25% all across the Mach number and angle of attack range. Base pressure measurements indicated that in the low Mach number range pressure rise occured. However, in the high transonic Mach number range, even though the force measurements showed drag reduction, there was no significant rise in base pressure. Ventilation showed delay in transonic drag rise. It is therefore suggested that the overall pressure field is modified by ventilation, which results in drag reduction of the configuration.

Keywords *: Bluff body drag reduction, Natural ventilation*

Symbols

L = Length of the configurations (1.5795 in)
M = Freestream Mach number
CN = Normal force coefficient, (Normal force/qA_{Ref})
CAF = Forebody axial force coefficient (CAT - CAB)
CAT = Axial force coefficient (Measured axial force/ qA_{Ref})
CAB = Base drag coefficient (CPB * S/A_{Ref})
CPB = Base pressure coefficient (Pb - Ps/q)
CPM = Pitching moment coefficient about nose
psid = Differential pressure with respect to atmospheric pressure
N1, N2 = Normal force measuring elements of the balance
S1, S2 = Side force measuring elements of the balance
AF = Axial force measuring element of the balance
RM = Rolling moment measuring element of the balance
q = Free stream dynamic pressure
S = Base area (in^2) of each configuration
Pb = Static pressure measured at model base
Po = Free stream total pressure, measured in the wind tunnel settling chamber
Ps = Free stream static pressure
α = Angle of attack
ΔCN = Uncertainty in CN
ΔCPM = Uncertainty in CPM
ΔCAF = Uncertainty in CAF
A_{Ref} = Base area of the basic model (3.043 in^2)

Paper Code : V63 N4/727-2011. Manuscript received on 28 Jul 2010. Reviewed and accepted as a Full Length Contributed Paper on 03 Aug 2011

L_{Ref} = Diameter of the individual configuration (1.9685 in to 2.4240 in)

XCPN/L = Location of center of pressure, -CPMα/CNα in the range of α ±4°

Introduction

The concept of natural ventilation of a bluff body such as a sphere was introduced [Suryanarayana et. al, 1993] where it was shown that by interconnecting the stagnation and base regions of a sphere, an internal ventilation, which adds mass, momentum and energy into the near wake of the sphere could be set up. Drag measurements in the Reynolds number range 65,000 to 7×10^5 have shown that whereas a small reduction of drag occurs in the subcritical range, a very significant reduction of drag, as much as 65% occurred in the supercritical range. Subsequently, detailed surface pressure measurements [Suryanarayana et. al, 1995] in the above Reynolds number range indicated that while there was no significant change in the external pressure distribution over the sphere in the subcritical Reynolds numbers, a substantial rise in the base pressures occurred at supercritical Reynolds numbers. This base pressure rise led to a kind of "base thrust", leading to drag reduction. Measurements of velocity fluctuations in water and wind tunnels using hot film and hot wire probes have clearly showed [Suryanarayana et. al, 2000, 1995] that while there was no noticeable change in the vortex shedding characteristics due to ventilation of a sphere at subcritical Reynolds numbers, there was a very substantial reduction in the velocity fluctuations at several sections across the near wake at supercritical Reynolds numbers, suggesting stabilization of the wake flow due to ventilation. Detailed visualizations of the surface flow patterns, wake flow using a laser light sheet, static and total pressure measurements along and across the ventilation duct as well as in the wake have shown [Suryanarayana, 1995] that the flow past a vented sphere at supercritical Reynolds numbers becomes more symmetric, as shown by the mean laminar separation, transitional/turbulent shear layer reattachment and turbulent boundary layer separation lines.

The occurrence of laminar separation bubble and the range of Reynolds number where this occurs were hardly altered, but the skewness of these lines and random oscillations of the near-wake associated with the basic (unvented) flow past a sphere [Taneda, 1978] at supercritical Reynolds numbers were removed by natural ventilation. Wake measurements showed that at supercritical Reynolds numbers, the near wake is split by the vent jet, resulting in the formation of a pair of vortex rings suggestive of a closed wake, as against the randomly rotating three-dimensional horseshoe vortex structure observed by Taneda [1978]. Studies on ventilation have been extended to higher Reynolds numbers by Mei Lu et. al [1998], wherein drag reduction of 40% with ventilation have been measured up to Reynolds number of 4.5×10^6. Jeon, et. al [2004] have shown that active forcing of the flow past a sphere by alternate blowing and suction at frequencies above a certain critical frequency, leads to drag reductions of the order of 50% at subcritical Reynolds numbers.

Few attempts have been reported in the literature to extend the concept of natural ventilation to stretched 3-dimensional bluff bodies, as shown by Grosche et. al [2001] and Falchi et. al [2006]. These studies suggest that as the body length is increased for a given diameter, there is a progressive reduction in the drag benefit due to ventilation. However, this result is not surprising since the skin friction drag takes over the pressure drag.

On two-dimensional bluff bodies, the effect of natural ventilation was first reported by Igarashi [1978] through measurements of vortex shedding frequency behind slotted circular cylinders in the Re no. range 13800 to 52000. The slot incidence with respect to the mean flow direction was varied and the nature of the base flow characterized into three regimes where the slot incidence was in the range 0 to 45°, 45° to 60° and 60° to 90°. Drag reduction of as much as 30% was reported in the first regime. Interferograms confirming some of these observed flow features were reported by Suryanarayana et. al [2005]. A comprehensive review of most of the recent papers on the topic of natural ventilation is covered by Suryanarayana [2009]. In the present studies, the effects of flare angle on the aerodynamic force and moment characteristics of a typical bluff body re-entry configuration featuring a blunt nose, a short cone and a flare are reported from measurements in a transonic wind tunnel.

Experimental Facility

Tests were conducted in the 0.6m transonic blowdown wind tunnel at the National Aerospace Laboratories, Bangalore, India. The test section has dimensions of 0.6m x 0.6m and Mach number capability from 0.2 to 1.2 and is provided with slots. The open area ratio of slots is 6% on top and bottom walls and 4% on side walls. Subsonic Mach numbers are achieved by choking the second throat downstream of the test section. Transonic Mach number control is provided by using control flaps at the downstream ends of top and bottom walls. The test Reynolds

number varied with the Mach number in the range 0.4 million to 1.4 million based on the model base diameter. Test Mach number was varied in the range 0.4 to 1.2.

Model Details

The axisymmetric bluff body model along with the support system is illustrated in Figs.1a and 1b. It features a main forebody to which several replaceable flares can be attached. The forebody has a hemispherical nose, which is tangentially matched to a 20° cone (first cone). A frustum of 25° cone (second cone, referred to as flare) is attached to the first cone, and the configuration referred to as Basic. For parametric studies, flares of 30°, 35° and 40° angles were chosen, to study the effect of flare angle on the longitudinal stability of the configuration; these are referred to as F30, F35 and F40 configurations. In addition, a 35° flare with provision for boundary layer ventilation (referred to as F35V) was designed and fabricated. The vented body has an annular slot of 1mm height at the junction between the first and second cones; the two parts are joined by thin webs at four discrete locations 90° apart. Thus, in the vented configuration, the flare resembles an annular wing. The models being bodies of revolution, the radius of the body along the longitudinal axis is represented by the equations given in Fig.1b. It may be noted that the length of the body is identical for all the configurations. The overall length of the body is less than the maximum diameter, a feature of bluff bodies. For force measurements using an internal strain gauge balance, it is necessary to enclose the entire balance inside the model to ensure a satisfactory surface contact. In the present case, since the length of the body is inadequate for this purpose, the base of the model is extended to the required length. The forebody and the extended base are integrally constructed and equipped with an inner sleeve made from EN 24 steel reamed to suit the balance, as shown in Fig.1a. An annular gap of 1mm was maintained between the outer diameter of the sleeve and the inner diameter of the shroud, to cater for elastic deflection of the model during wind tunnel tests.

The models were made using ABS plastic, using Fusion Deposition Moulding technique; the models had a rough finish because of the staircasing effect that arises during the manufacturing process. Since the contribution of skin friction to the overall drag of bluff bodies is quite small [Achenbach, 1974], the model surface was not smoothened. Typical differences between the specified and inspected dimensions of the body were within ± 0.6 mm, which occurred around the maximum diameter of the body. The models were manufactured at APDAP, Department of Mechanical Engineering, Indian Institute of Science, Bangalore. Fig.2 shows all the components of the model.

Instrumentation

A 0.75" diameter 6-component ABLE balance was used for the force measurements. The balance was mounted using a long sting and S elements (S1 and S2) used for normal force measurement. Total and static pressures in the wind tunnel were measured using ±15 psid and ±10 psid pressure transducers respectively. Base pressures behind the model were measured at four diametrically opposite locations (0°, 90°, 180° and 270° with respect to the pitch plane as shown in Fig.3b) using $\pm$ 10 psid pressure transducers. The measured base pressures were used to compute the base drag coefficients and subtracted from the measured total drag coefficients to obtain the forebody drag of the configuration. The balance load ranges are: N1 = N2 = 300 Lb., S1 = S2 = 100 Lb., AF = 60 Lb., RM = 60 in-Lb. Uncertainties in the aerodynamic coefficients, based on $\pm 0.1\%$ of the balance capacity are: $\Delta CN = \pm 0.0215$; $\Delta CPM = \pm 0.095$; $\Delta CAF = \pm 0.004$.

Results and Discussions

Effect of increasing the Flare Angle

Figures 4 and 5 show the effect of increasing the flare angle from 25° to 40° on the variations of CN and CPM with α at a freestream Mach number of 0.80. Systematic decreases in both the normal force as well as pitching moment are seen. The reductions in slopes $CN\alpha$ and $CPM\alpha$ are about 38% and 35% respectively at M = 0.80. It seems likely that this loss is due to increasing extents of flow separation, caused at the junction between the first cone and the flare, with a possible flow reattachment somewhere on the flare. As shown in Fig.6, as the flare angle is increased, systematic increase in the axial force is observed. The increase in axial force with increased flare angle is not surprising since the base diameter increased with the flare angle, as shown in Table-1.

Variations of $CN\alpha$ and $CPM\alpha$ with free stream Mach number are shown in Figs.7 and 8. The reduction in both

Table-1 : Base Diameters of Various Models Tested

Configuration	Basic	F 30	F 35	F 35 V	F 40
Base Diameter (mm)	50	53.51	57.41	57.41	61.85

these quantities is observed at all the Mach numbers tested. The center of pressure, obtained as the ratio of $CPM\alpha/CN\alpha$ in the range of $\alpha \pm 4°$ shows a systematic shift towards the nose, as shown in Fig.9, suggesting that the decreasing contribution of the flare normal force as a function of flare angle is the cause.

Effect of Natural Ventilation

Ventilating the 35° flare does not show significant changes in normal force and pitching moment characteristics as compared to the unvented 35° flare at M =0.80 (Figs.4 and 5). However, significant reduction in the drag coefficient, of 37% is seen with ventilation at M = 0.80 (Fig.6). As shown in Figs.7 and 8, small reductions in the slopes of $CN\alpha$ and $CPM\alpha$ with free stream Mach number are seen with ventilation. Fig.9 shows that the configuration becomes less stable with ventilation. However, the most significant effect of natural ventilation appears to be on the drag coefficient. As shown in Fig.10, the drag coefficient of the vented body is about 40% lower than that of the unvented body of the same base diameter, all across the Mach numbers tested. It may be noted that as shown in Table-1, the base area of the vented configuration (F 35V) is about 32% higher than that of the basic configuration. Nevertheless, its drag coefficient is 20 to 25% less, especially for M > 1.0. It is further noted from Fig.10 that the transonic drag rise for the vented body is delayed by ventilation.

In order to understand the possible reasons for drag reduction, it is useful to consider the flow structure in the base of a vented sphere. As shown in Fig.11, formation of a closed recirculation zone due to interaction between inner and outer shear layers surrounding the flare may be expected to increase the base pressure, which in turn reduces the base drag and consequently the total drag. A possible flow topology, which explains the base pressure rise at the flare is described in Fig.12. The viscous layer at the cone-flare junction is vented into the near wake as the inner shear layer and forms a closed recirculation region along with the external shear layer. Consequently, a pair of counter-rotating vortices forms at the flare base, leading to base pressure rise. Measurements of base pressure at M = 0.80 confirm the base pressure rise (Fig.13). However, such a base pressure rise was not observed consistently at all Mach numbers, whereas drag measurements confirm the drag reduction at all Mach numbers. For example, at M = 1.16, base pressure showed a marginal decrease with ventilation (Fig.14), whereas the drag coefficient showed a clear decrease. It must however be noted that the ratio of the effective sting diameter to the model base diameter is quite high in the present experiments because of the need to shield the extended portion of the model from the freestream. At transonic conditions, the base pressure can be significantly affected by the larger sting diameter. Further experiments, with a bigger model and thinner sting diameter are necessary to confirm the base pressure changes with ventilation. However, the actual force measured by the balance does indicate drag reduction with ventilation.

Acknowledgments

The author acknowledges with thanks the support provided by Director, National Aerospace Laboratories, Bangalore in carrying out the reported studies. The contribution of Mr K. S. Raman, former Scientist, National Aerospace Laboratories, who sadly passed away during the course of reported studies is remembered with thanks. Useful discussions with Mr G. Rajendra, Emeritus Scientist, NAL, assistance of the staff of NAL 0.6m Wind Tunnel and Head, NTAF in conducting the tests are acknowledged with thanks.

References

1. Suryanarayana, G.K., Henning Pauer and Meier, G.E.A., "Bluff-body Drag Reduction by Passive Ventilation", Experiments in Fluids, Vol.16, No. 2, pp. 73-81, 1993.

2. Suryanarayana, G.K. and Meier, G.E.A., "Effect of Ventilation on the Flowfield Around a Sphere", Experiments in Fluids, Vol.19, No.2, pp.78-88, 1995.

3. Suryanarayana, G.K. and Prabhu, A., "Effect of Natural Ventilation on the Boundary Layer Separation and Near-wake Vortex Shedding Characteristics of a Sphere", Experiments in Fluids, Vol.29, No.6, pp. 582-591, 2000.

4. Suryanarayana, G.K., "On the Reduction of Drag of a Sphere by Natural Ventilation, Dissertation", Department of Aerospace Engineering, Indian Institute of Science, Bangalore, India, 1995.

5. Suryanarayana, G.K., "Aerodynamic Drag Reduction of Bluff Bodies: Application of Natural Ventilation", Lambert Academic Publications, Germany, ISBN 978-3-8383-1103-6, 2009.

6. Taneda, S., "Visual Observations of the Flow Past a Sphere at Reynolds Numbers Between 10^4 and 10^6". Journal of Fluid Mechanics, Vol. 85, Part-1, pp.187-192, 1978.

7. Lu, M., Grosche, F.R. and Meier, G.E.A., "Drag Reduction of a Sphere at Supercritical Reynolds Numbers Using Passive Ventilation", IUTAM-Symposium on Mechanics of Passive and Active Flow Control, 1998.

8. Sejeong Jeon., Jin Choi., Woo-Pyung Jeon., Heachon Choi and Jinil Park., "Active Control of Flow Over a Sphere for Drag Reduction at Subcritical Reynolds Number", Journal of Fluid Mechanics, Vol.517, pp.113-129, 2004.

9. Grosche, F.R. and Meier, G.E.A., "Research at DLR Gö ttingen on Bluff Body Aerodynamics, Drag Reduction by Wake Ventilation and Active Flow Control", Journal of Wind Engineering and Industrial Aerodynamics, Vol.89, Issues 14-15, pp.1201-1218, 2001.

10. Falchi., Provenzano,G., Pietrogiacomi, D. and Romano, G.P., "Experiments and Numerical Investigation of Flow Control on Bluff Bodies by Passive Ventilation", Experiments in Fluids, Vol.41, No.1, pp.21-33, 2006.

11. Igarashi., "Flow Characteristics Around a Circular Cylinder with a Slot Bull", JSME 21 154, pp.656-664, 1978.

12. Suryanarayana, G.K., Meir, G.E.A. and Henning Pauer., "Vented Circular Cylinder as a Vortex Generator", Journal of Visualization, Vol.8, No.3, 2005.

13. Achenbach, E., "The Effects of Surface Roughness and Tunnel Blockage on Flow Past Spheres". Journal of Fluid Mechanics, Vol.65:1, pp.113-125, 1974.

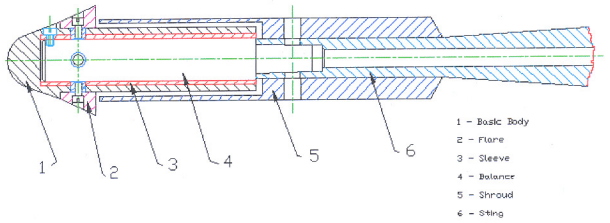

Fig.1a A Sketch of the Model

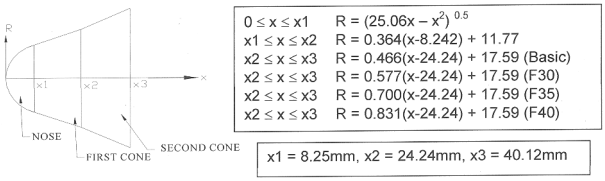

Fig.1b Geometric Details of the Model

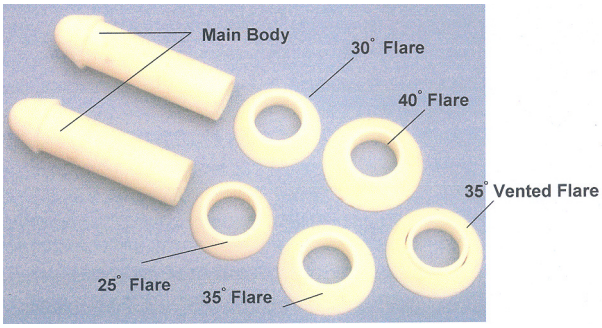

Fig.2 Photograph of Model Components

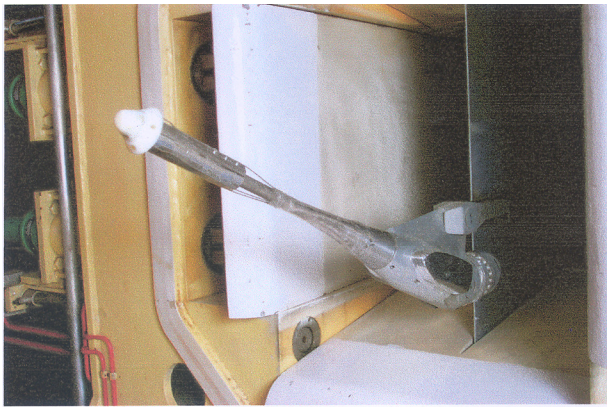

Fig.3a Photograph of Model Mounted in the 0.6m Wind Tunnel

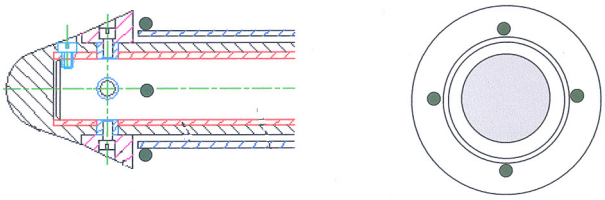

Fig.3b Location of Base Pressure Probes

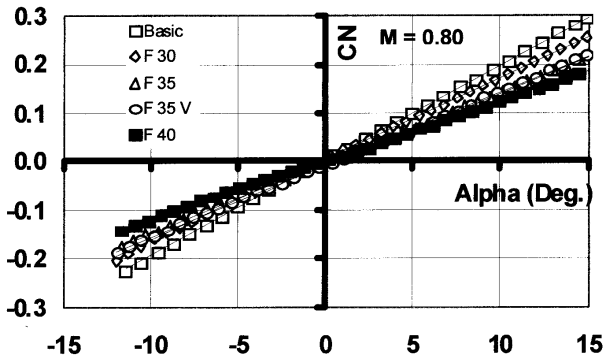

Fig.4 Effect of Flare Angle on the Variation of CN with α

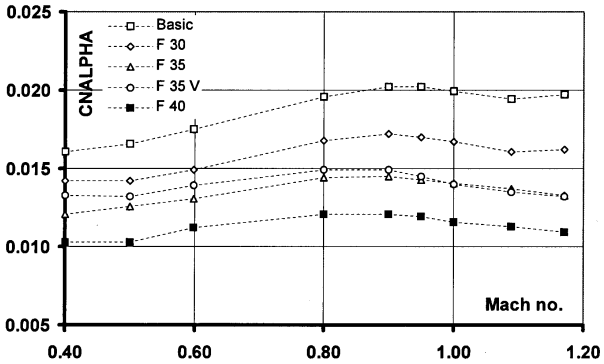

Fig.7 Effect of Mach Number on the Variations of CNα

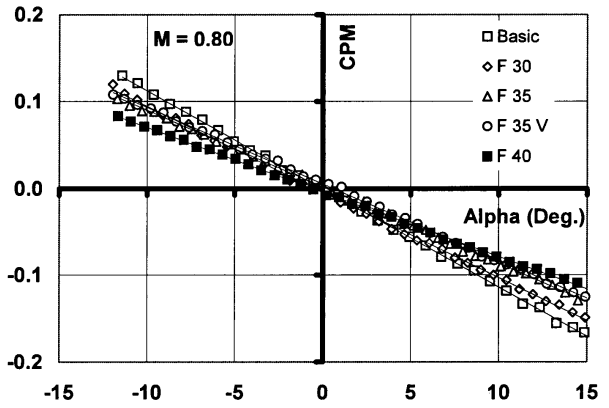

Fig.5 Effect of Flare Angle on the Variation of CPM with α

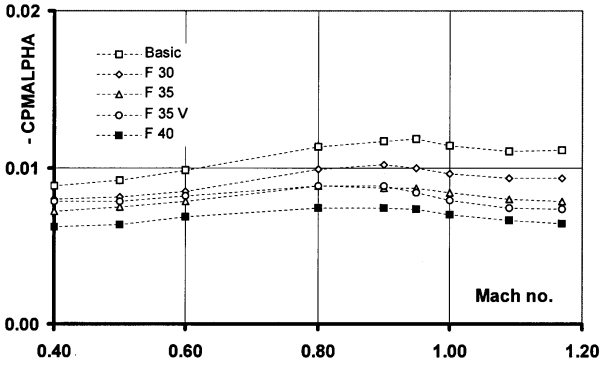

Fig.8 Effect of Mach Number on the Variations of CPMα

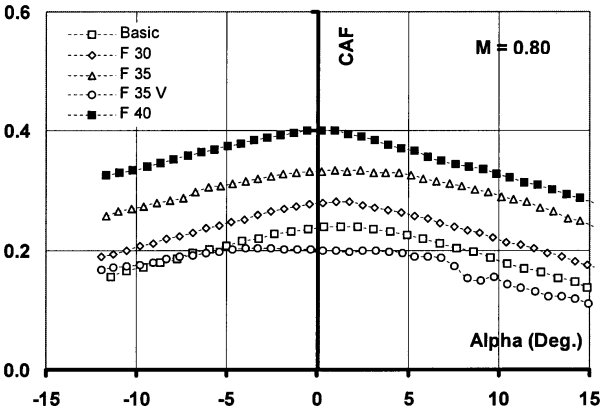

Fig.6 Effect of Flare Angle on the Variation of CAF with α

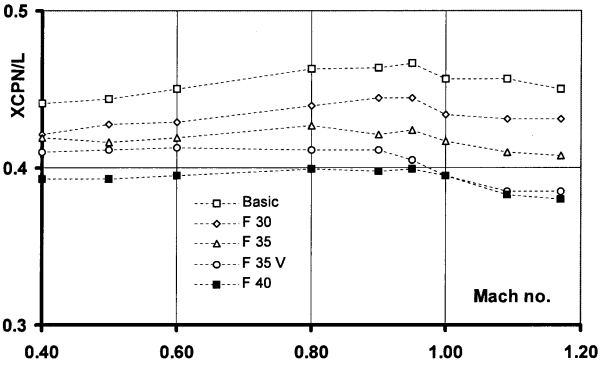

Fig.9 Effect of Mach Number on the Variations of Center of Pressure

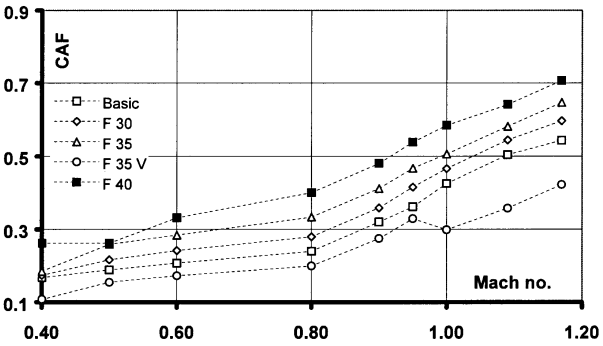

Fig.10 Effect of Natural Ventilation on Drag Coefficient

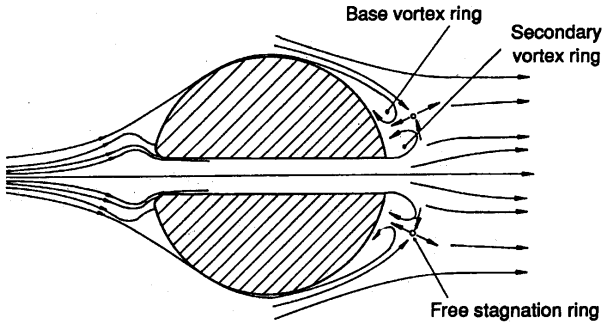

Fig.11 The Wake Structure Behind a Vented Sphere at High Re (2, 3, 4)

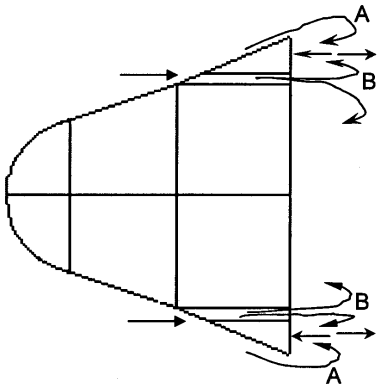

A Outer shear layer

B Inner shear layer

Fig.12 The Wake Structure Due to Natural Ventilation of Flared Body

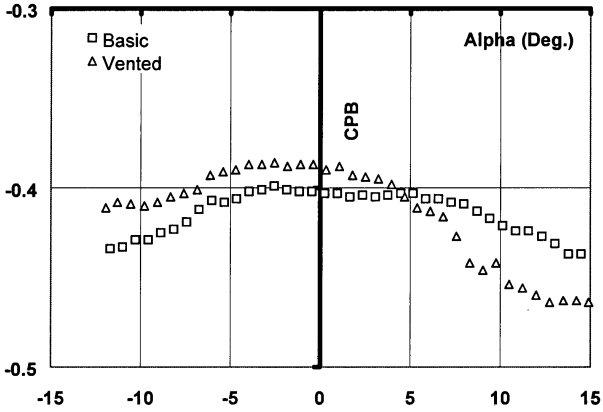

Fig.13 Effect of Ventilation on the Base Pressure at M = 0.80

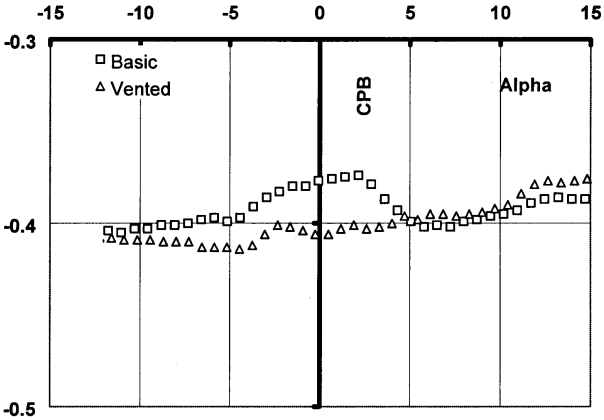

Fig.14 Effect of Ventilation on the Base Pressure at M = 1.16